Application of density functional theory calculations to the statistical mechanics of normal and anomalous melting

Sven P. Rudin, Nicolas Bock, and Duane C. Wallace

Phys. Rev. B **90**, 174109 — Published 20 November 2014

DOI: 10.1103/PhysRevB.90.174109

Application of Density Functional Theory Calculations to the Statistical Mechanics of Normal and Anomalous Melting

Sven P. Rudin, Nicolas Bock, and Duane C. Wallace
Los Alamos National Laboratory, Los Alamos, New Mexico 87545, USA
(Dated: September 29, 2014)

Density functional theory (DFT) calculations reliably aid in understanding the relative stability of different crystal phases as functions of pressure and temperature. Our purpose here is to employ DFT to analyze the character of the melting process, with an emphasis on comparing normal and anomalous melting. The normal–anomalous distinction is the absence or presence, respectively, of a significant electronic structure change between crystal and liquid. We study the normal melters Na and Cu, which are metallic in both phases, and the anomalous melter Ga, which has a partially covalent crystal and a nearly-free-electron liquid. We calculate free energies from lattice dynamics for the crystal and from vibration-transit (V-T) theory for the liquid, where the liquid formulation is similar to that of the crystal but has an additional term representing the diffusive transits. Internal energies U and entropies S calculated for both phases of Na and Cu were previously shown to be in good agreement with experiment, here we find the same agreement for Ga. The dominant theoretical terms in the melting ΔU and ΔS are the structural potential energy, the vibrational entropy, and the purely liquid transit terms in both U and S. The melting changes in structural energy and vibrational entropy are much larger in Ga than in Na and Cu. This behavior arises from the change in electronic structure in Ga, and is the identifying characteristic of anomalous melting. We interpret our DFT results in terms of the physical effects of the relatively few covalent bonds in the otherwise metallic Ga crystal.

PACS numbers: 64.70.D-, 64.60.A-, 64.60.Cn, 64.60.Ej

I. INTRODUCTION

Density functional theory (DFT) calculations offer a reliable means to explore phase diagrams of condensed matter systems across large regions of pressure and temperature. The calculations deliver reasonably sound phase boundaries and an improved understanding of changes in both crystal structure and electronic structure – as well as how the two relate (see for example Ref. 1). The exploration relies on examining relevant portions of the potential energy surface, Φ, given by the electronic ground state as a function of the nuclear configuration. The subset of configurations given by local equilibria suffices to study pressure-induced phase changes for systems at zero temperature (neglecting zero-point energy). As a result, advances have been more forthcoming along the pressure axis than on the temperature axis. The inclusion of phonons, given by the local curvature of Φ, converts the local equilibria description into the quasi-harmonic approximation and enables the study of temperature-induced phase transitions.[2] To date, this approach has focused on solid–solid transitions; here we apply it to the solid–liquid transition, melting, for which DFT studies heretofore have relied on molecular dynamics (MD).

Important advances along the pressure axis at low temperature have been made in recent years, in particular for light element systems, revealing new structures with unusual electronic properties. DFT calculations by Neaton and Ashcroft found Li to undergo a symmetry breaking distortion to a paired ground state that contrasts with the intuitive expectation of nearly free electron behavior.[3] X-ray diffraction measurements by Hanfland *et al.* confirm that Li undergoes pronounced structural changes under pressure.[4] DFT calculations by Feng *et al.* found the electronic DOS of LiBe alloy shows a remarkable quasi-two-dimensional electronic structure that arises from a planar arrangement of valence electrons promoted from the Li cores.[5] From a study of the structural competition as function of volume in Group IIIA elements, Simak *et al.* found that the structure-determining mechanism originates in the degree of *s*-*p* mixing of valence electrons.[6,7] This mixing governs the stability of B, Al, Ga, In and Tl at zero pressure,[7] and also qualitatively accounts for high pressure phase transitions in B and Ga and predicts similar behavior for In.[6]

Pressure induced electronic structure changes, and the crystal structure transitions they drive, have consequences at elevated temperatures. The ultimate reason is that the electronic structure controls both structural and nuclear-motional properties of condensed matter. For highly compressed Na, Neaton and Ashcroft predicted transformations from the symmetric, metallic phase to low symmetry crystal structures that possess semi metallic behavior and tend ultimately to be semiconducting.[8] Such transformations were confirmed by X-ray measurements to 120 GPa by Hanfland *et al.* and by Syassen.[9,10] The melting curve $T_m(P)$, measured by Gregoryanz *et al.*,[11] shows a normal increase from 371 K at $P = 0$ to 1000 K at around 30 GPa, then a downturn and subsequent decrease of T_m all the way to 300 K at around 120 GPa. This remarkable behavior was accounted for by MD calculations by Raty *et al.*,[12] which also showed that the liquid undergoes electronic structure changes analogous to those in the solid.

The change in the melting curve of Na from positive to negative slope signals a change in the melting process from normal to anomalous. This melting classification goes back to a study of the melting of elements, where experimental data for the entropy difference between liquid and crystal at a common volume were found to lie in two well-separated distributions.[13] The constant volume specification is important because it separates out thermal expansion effects and puts the focus on the intrinsic liquid–crystal disordering effect. The resulting physical interpretation is that normal melting elements have qualitatively the same electronic structure in the liquid and crystal at a common volume, while anomalous melting elements have a significant liquid-crystal electronic structure difference.[13] We shall employ DFT calculations to examine both of these melting processes in this work.

The advance that allows us to apply DFT calculations to solid–liquid phase transitions on the same footing as solid–solid phase transitions is a description of liquids that closely resembles that of solids: vibration-transit (V-T) theory. In V-T theory the liquid has a representative structure, and has nuclear motion in the form of vibrations about the structure plus transits that carry the system rapidly among structures. At present the structural and vibrational parameters are accessible to DFT calculations, while the small transit contribution is treated by a statistical mechanical model. For Na and Cu at melt this procedure shows excellent agreement with experiment for the equilibrium volume, the bulk modulus, the entropy and internal energy, for crystal and liquid alike.[14] Our purpose here is to formulate the melting transition in terms of characteristic structural and nuclear-motional properties of the two phases in a single theory for both normal and anomalous melting. We shall carry out this program for Na and Cu (normal) and Ga (anomalous) at zero pressure where highly accurate experimental data are available.

Ga has long been known for its electronic structure difference between the α-Ga crystal and the liquid phase (l-Ga). That l-Ga is unlike α-Ga, but similar to the slightly more dense β-Ga, was suggested by measured pair distribution functions,[15] by diffuse neutron scattering,[16] and by measured elastic constants and bulk modulus.[17,18] The presence of a pseudo gap in the electronic DOS of α-Ga was attributed by Heine to a partial covalence;[19,20] that the pseudo gap is missing in l-Ga was observed by Hafner and Jank;[21] and Gong *et al.* concluded from electronic structure calculations that α-Ga contains covalent dimers held together by metallic forces.[22] A picture sufficient for discussion here is that l-Ga is a nearly free electron (NFE) metal, while each atom in α-Ga is one member of a covalent pair bond, with these bonds connecting parallel metallic sheets (see Sec. IV of Voloshina *et al.*,[23]; Fig. 1 in Lyapin *et al.*,[18]; Fig. 31-2

in Donohue,[24]). DFT calculations on Ga, outlined at the beginning of Sec. IV, agree with these observations and provide additional insight.

Our needed statistical mechanical equations, along with a sketch of the V-T formalism, is provided in Sec. II. In order to relate theory more directly to experiment, the original melting-of-elements study (Ref. 13) is transformed from a constant-volume to a constant-pressure formulation in Sec. III. Sec. IV compares theory and experiment for the entropy $S(V,T)$ and the internal energy $U(V,T)$ (where V is volume and T is temperature) of α-Ga and l-Ga at melt, and analyzes the melting process for Na, Cu, and Ga. Sec. V provides a summary of conclusions and a description of melting in terms of the structural potentials and nuclear motions of the equilibrium phases at melt.

DFT calculations of electronic and vibrational properties of α-Ga and l-Ga are presented in the online Supplemental Material, and the technique for finding and testing the liquid structure is demonstrated.[25]

II. STATISTICAL MECHANICS OF V-T THEORY

V-T theory begins with the hypothesis that among the many body potential energy valleys those with a random structure dominate the liquid statistical mechanics, and that every such valley has the same statistical mechanics properties in the thermodynamic limit.[26–28] The nuclear motion consists of many body vibrational motion in one (any) random valley, interspersed with transits, which are collective motions of small nuclear clusters that carry the system between random valleys. The vibrational Hamiltonian represents a single random valley harmonically extended to infinity, so that all vibrational statistical mechanics can be expressed in closed form. Thermodynamic functions are roughly 90% vibrational and 10% transit.

In V-T theory for the liquid (quantities for liquid are denoted with a superscript l), vibrations (vib), transits (tr), and electronic excitations (el) contribute to the entropy

$$S^l(V,T) = S^l_{vib}(V,T) + S_{tr}(V,T) + S^l_{el}(V,T), \tag{1}$$

and the internal energy

$$U^l(V,T) = \Phi^l_0 + U^l_{vib}(V,T) + U_{tr}(V,T) + U^l_{el}(V,T). \tag{2}$$

Φ^l_0 is the random structure potential energy. For all elements heavier than He, the nuclear motion is approximately classical at $T \gtrsim T_m$, so the high temperature expansions are appropriate:

$$S^l_{vib}(V,T) = 3k_B \left\{ \ln\left[T/\theta^l_0(V)\right] + 1 + \frac{1}{40}\left[\theta^l_2(V)/T\right]^2 + ... \right\}, \tag{3}$$

$$U^l_{vib}(V,T) = 3k_B T \left\{ 1 + \frac{1}{20}\left[\theta^l_2(V)/T\right]^2 + ... \right\}. \tag{4}$$

$\theta^l_0(V)$ and $\theta^l_2(V)$ are simply related to the logarithmic moment and second moment, respectively, of the normal mode frequency distribution (see pp. 149–152 of Ref. 26). The leading terms express classical statistical mechanics, while the series in powers of T^{-2} provide the (small) quantum corrections.

The transit contributions in Eqs. (1) and (2) are $S_{tr}(V,T)$ and $U_{tr}(V,T)$, respectively. The superscript l is omitted because these terms are present only in the liquid state. Our transit model has been substantially improved in recent years. An analysis of experimental entropy data for elemental liquids revealed the scaling property,[27]

$$S_{tr}(V,T) = S_{tr}(T/\theta_{tr}(V)), \tag{5}$$

where $\theta_{tr}(V)$ is a transit characteristic temperature for each element. The theory was completed with a statistical mechanics model for the transit free energy $F_{tr}(V,T)$.[28] Because $F_{tr}(V,T)$ belongs entirely to the liquid, it is insensitive to the crystal and to the melting process.

The electronic excitation contributions express the thermal excitation of electrons from their ground state. These are calculated from the electronic density of states (DOS) $n(\epsilon)$, and for the present study we need only the leading Sommerfeld approximation,

$$S^l_{el}(V,T) = \Gamma^l(V)T, \tag{6}$$

$$U^l_{el}(V,T) = \frac{1}{2}\Gamma^l(V)T^2, \tag{7}$$

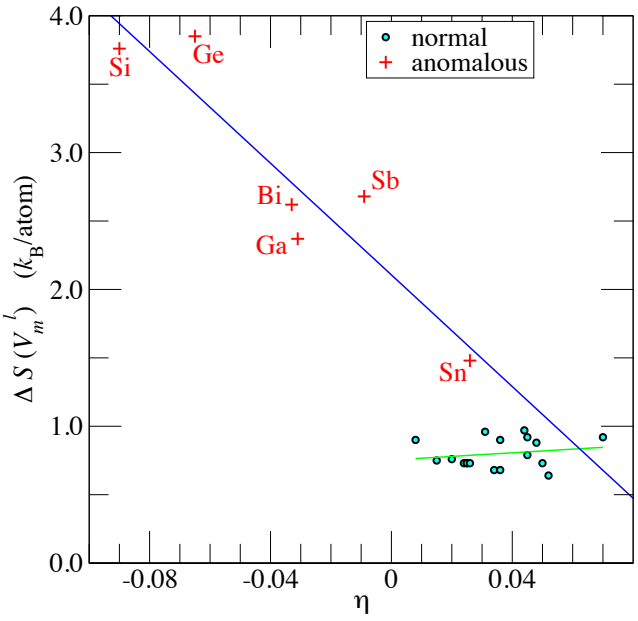

FIG. 1. (color online) Experimental data for the liquid-crystal entropy difference at the common volume V_m^l, against the relative volume change on melting, η. The lines are independent least-squares fits to the two distributions.

where

$$\Gamma^l(V) = \frac{1}{3}\pi^2 k_B^2 n^l(\epsilon_F), \tag{8}$$

with ϵ_F the Fermi energy. In comparison, for transition metals with partially filled d bands accurate calculations of the electronic excitation contributions at T_m requires an integration over $n(\epsilon)$.[29]

For the crystal (quantities for crystal are denoted with a superscript c), we use quasiharmonic lattice dynamics theory.[26,30] The thermodynamic functions are formally the same as in Eqs. (1) and (2), with the transit contributions omitted:

$$S^c(V,T) = S^c_{vib}(V,T) + S^c_{el}(V,T), \tag{9}$$

$$U^c(V,T) = \Phi^c_0 + U^c_{vib}(V,T) + U^c_{el}(V,T). \tag{10}$$

The vibrational formulas are again Eqs. (3) and (4), with the crystal parameters $\theta^c_0(V)$ and $\theta^c_2(V)$ in the place of the liquid parameters. The crystal electronic excitation formulas are Eqs. (6)-(8) based on the crystal DOS, $n^c(\epsilon)$.

III. ANALYSIS OF THE EXPERIMENTAL, $P = 0$ MELTING ENTROPY

The entropy of melting at $P = 0$ is denoted $\Delta S(P = 0)$, and is the quantity measured in the laboratory. The relative volume change on melting is η,

$$\eta = \frac{V_m^l - V_m^c}{V_m^l}. \tag{11}$$

$\Delta S(P = 0)$ is decomposed into two terms: $\Delta S(V_m^l)$ is the liquid-crystal entropy difference at the common volume V_m^l, and the volume change contribution is calculated to first order in η, to give (see Ref. 13)

$$\Delta S(P = 0) = \Delta S(V_m^l) + \left.\frac{\partial S}{\partial \ln V}\right|_{T_m} \eta. \tag{12}$$

$(\partial S/\partial \ln V)_{T_m}$ is obtained from experimental data for the crystal at melt, because accurate data are more readily available for crystal than liquid. Eq. (12) is used to extract the intrinsic $\Delta S(V_m^l)$ from the experimental $\Delta S(P = 0)$.

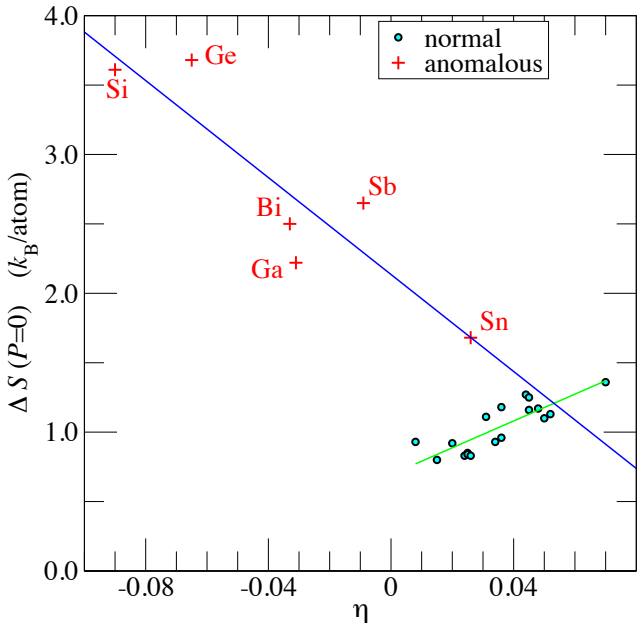

FIG. 2. (color online) Experimental data for the entropy of melting at $P = 0$ for the elements shown in Fig. 1. Data for normal melters Li, Na, K, Rb, Cs, Ba, Cu, Ag, Au, Cd, Hg, In, Pb, Fe, Ni and for the anomalous melters (Sn, Ga, Sb, Bi, Si, Ge) are from Hultgren *et al.*;[31] data for Mg, Zn, and Al are from Chase *et al.*[32]

Highly accurate experimental data for $\Delta S(V_m^l)$ for 18 normal melting and 6 anomalous melting elements are listed in Table 22.1 of Ref. 26. Compared to this tabulation of data, a strong enhancement of the distinction between normal and anomalous distributions is obtained by graphing $\Delta S(V_m^l)$ against the experimental η in Fig. 1. The normal distribution has mean $0.80k_B$, and has no significant η dependence. Following the discussion in Sec. II, the mean is now encoded in the transit free energy, and much of the scatter in the normal distribution points is now accounted for by the transit scaling temperature $\theta_{tr}(V)$ for each element (see Eq. (5)). Hence the normal distribution in Fig. 1 is entirely a liquid property.

In contrast to the character of the distribution for normal melters, the distribution for anomalous melters in Fig. 1 spans a very large range and has strong η dependence. These properties are due primarily to the electronic structure change between crystal and liquid, and cannot be assigned to the liquid alone.

An analysis at $P = 0$, in terms of the actual crystal and liquid states in the two-phase region, would be preferable in discussing experimental data. Figure 2 graphs the experimental $\Delta S(P = 0)$ against η for the same 24 elements shown in Fig. 1 and retains the same two distributions. Here, the normal melting distribution is the sum of two contributions, the $\Delta S(V_m^l)$ distribution from Fig. 1, representing transits, and the volume change contribution expressing the second term in Eq. (12), which imparts upon the normal distribution a slope.

The volume change contribution also provides a small change of slope between Figs. 1 and 2 for the anomalous melting elements. Because of the electronic structure change, it makes a difference whether the volume change term in Eq. (12) is assigned to crystal or liquid. Since that term is relatively small in anomalous melting, we shall leave this issue unresolved.

The character of the data in Fig. 2 will serve as a pattern for our analysis in the next section.

IV. ANALYSIS OF MELTING

Our analysis of melting relies on data calculated with DFT previously for Na and Cu[14] and here for Ga. Details of the calculations for Ga appear in the Supplemental Material,[25] and the results for α-Ga show good agreement with previous work by others (see, e.g., Ref. 23). Since this work reports the first application of DFT to V-T theory for an anomalous melter, we begin this section by reporting selected results from our calculations on Ga.

Figure 3 summarizes the significantly different character of Ga's liquid and solid phases. The partial covalence in α-Ga induces a pseudo gap in the electronic DOS, and the high-frequency vibrations of the covalent dimers appear in the vibrational DOS separated by a gap from the remaining vibrations. Both gaps disappear in the liquid phase; for the electronic DOS this occurs by a smoothing out of the DOS toward a more free-electron like character, for the

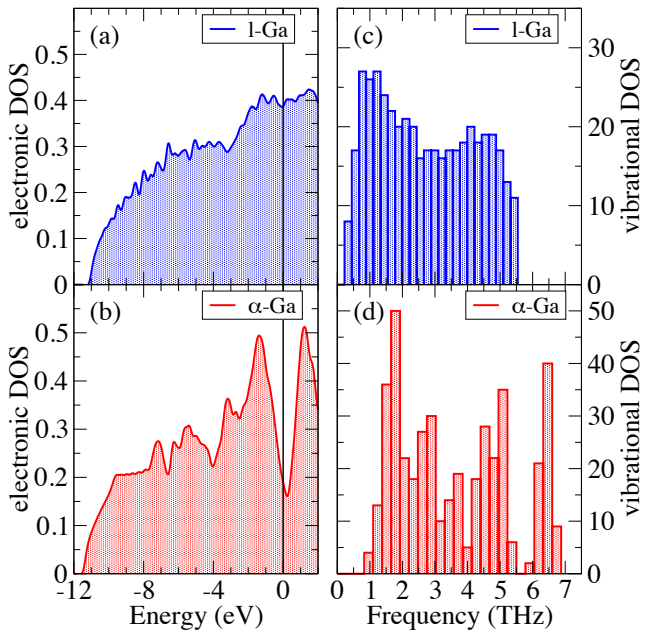

FIG. 3. (color online) Calculated electronic and vibrational densities of states (DOS) for Ga in solid and liquid phases at their respective measured melting volumes. The vibrational DOSs stem from evaluating the frequencies for all wave vectors commensurate with supercells containing $N = 144$ atoms for α-Ga and $N = 150$ atoms for liquid Ga.

Quantity	α-Ga	l-Ga
V_m (Å^3) (expt)	19.59	19.00
$E(V)$ (structure) meV	-3591.88	-3550.54
$(E^l - E^c)$ (meV)	41.34	
θ_0 (K)	154.2	106.3
θ_1 (K)	233. 0	171.8
θ_2 (K)	249.5	189.0
θ_{tr} (K)	—	360[a]
$n(\epsilon_F)$ (eV^{-1})	0.191	0.330
$\Gamma_{\rm el}$ (10^{-5} meV/K^2)	0.467	0.806
$S_{\rm vib}$ (k_B)	5.07	6.17
$S_{\rm tr}$ (k_B)	—	0.80
$S_{\rm el}$ (k_B)	0.02	0.04
Φ_0 (meV)	-21.9	19.4
$U_{\rm vib}$ (meV)	81.0	79.8
$U_{\rm tr}$ (meV)	—	10.0
$U_{\rm el}$ (meV)	0.2	0.4

[a] Ref. 27

TABLE I. For crystal and liquid Ga at $T_m = 302.9$ K and $P = 0$: The experimental volumes, the calculated Hamiltonian parameters, and the separate theoretical contributions to the total entropy and energy. The thermodynamic functions rely on quantities entirely calculated with DFT except for the measured volumes at melt, V_m, and the transit characteristic temperature, $\theta_{\rm tr}$, which is determined by statistical mechanics and experimental data.

vibrational DOS the high-frequency vibrations disappear along with the covalent dimers and their weight is subsumed into the lower spectrum of frequencies (which are also more evenly distributed).

From the markedly different DOS follow appreciably different Hamiltonian parameters, as reported in Table I. The calculated entropy and energy of the Ga phases at melt compare well with experiment, as shown in Table II, by way of Δ, the relative error of theory,

$$\Delta = \frac{\text{theory} - \text{experiment}}{\text{experiment}}. \tag{13}$$

Phase	Quantity	Theory	Experiment	Δ
α-Ga	$S^c(k_B)$	5.09	4.96	0.026
	U^c (meV)	59.3	59.1	0.003
l-Ga	$S^l(k_B)$	7.01	7.18	-0.024
	U^l (meV)	109.6	117.1	-0.064

TABLE II. For crystal and liquid Ga at $T_m = 302.9$ K and $P = 0$: Comparison of theory with experiment for entropy and internal energy.

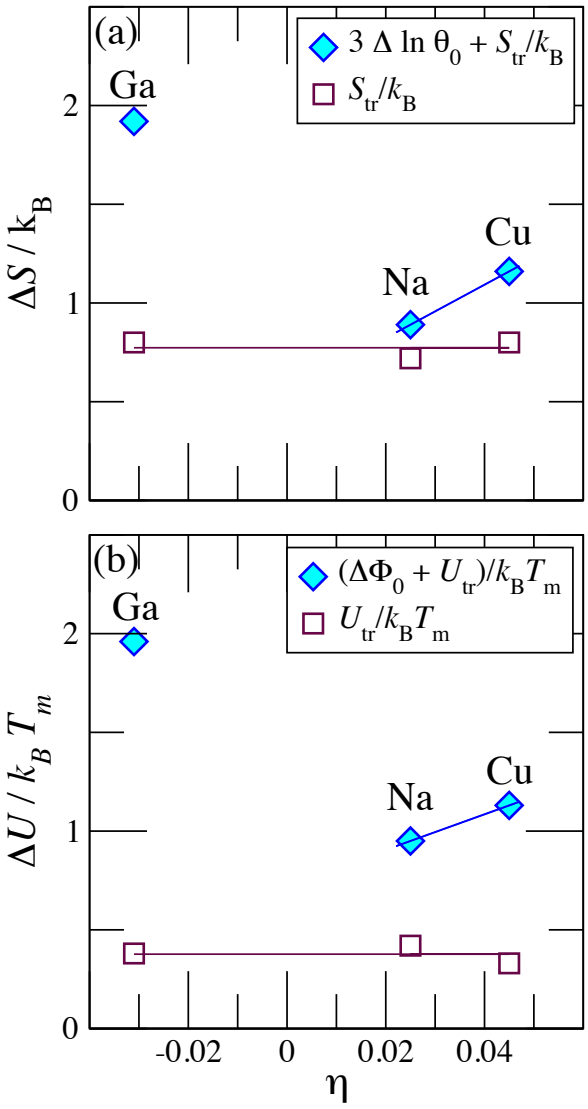

FIG. 4. (color online) Dominant theoretical contributions to $P = 0$ melting *vs.* η: (a) for the entropy and (b) for the energy. Open squares show transit contributions and filled diamonds show the total.

The Δ values are only a few times the estimated experimental errors,[31,32] and are extremely small even for DFT, except for the liquid internal energy, where the 6% error is still very good.

We now consider our complete list of test elements, Na, Cu, and Ga. The Hamiltonian parameters for Na and Cu, calculated from DFT, are listed in Table III; the corresponding entropy and energy data can be found in Ref. 14.[33] While we use the experimental $P = 0$ volume for Ga, the Na and Cu data are evaluated at the theoretical $P = 0$ volumes, the difference being insignificant for this analysis. We carry out our melting study in terms of theoretical results for energy and entropy contributions. In making comparisons among different elemental liquids,

Quantity	bcc-Na	l-Na	fcc-Cu	l-Cu
T_m (K)	370.87	370.87	1358	1358
V_m (Å^3)	39.79	40.93	13.05	13.54
θ_0 (K)	105.20	99.34	182.23	161.36
θ_1 (K)	152.34	144.42	252.02	238.82
θ_2 (K)	155.85	149.23	251.81	250.05
θ_{tr} (K)	—	570	—	1358
Φ_0 (meV)	-12.22	4.62	3.14	96.46

TABLE III. Na and Cu data collection.[14]

Quantity	Na	Cu	Ga
$\Delta S/k_B$ (theory)	0.89	1.16	1.92
$\Delta S/k_B$ (exp)	0.85	1.15	2.22
$\Delta U/k_BT_m$ (theory)	0.94	1.13	1.93
$\Delta U/k_BT_m$ (exp)	0.85	1.15	2.22
$\Delta F/k_BT_m$ (theory)	0.05	-0.03	0.01
$\Delta F/k_BT_m$ (exp)	0.00	0.00	0.00
S_{tr}/k_B	0.72	0.80	0.80
U_{tr}/k_BT_m	0.42	0.33	0.38
F_{tr}/k_BT_m	-0.30	-0.47	-0.42
$3\Delta \ln \theta_0$	0.17	0.36	1.12
$\Delta\Phi_0/k_BT_m$	0.53	0.80	1.58

TABLE IV. Comparison of theory with experiment for melting quantities at $P = 0$, and values of the dominant theoretical melting contributions (Eqs. (14) and (15)).

terms in $\Delta S/k_B$ can be compared directly, as in Figs. 1 and 2. Then, because of the $P = 0$ free energy constraint, $\Delta U = T_m\Delta S$, the ΔU terms are compared in the scaled form $\Delta U/k_BT_m$.

Table IV compares theory and experiment for the melting quantities at $P = 0$ to show the high level of theoretical accuracy in this analysis. The near zero value of the theoretical $\Delta F/k_BT_m$ is encouraging. Table IV also shows the stabilization of the liquid phase by the transit free energy.

Our first step is to identify the dominant contributions to $\Delta S(P = 0)$ and $\Delta U(P = 0)$ from the equations in Sec. II. In general, both the electronic excitations and the vibrational quantum corrections are insignificant in melting, being ~ 0.01 in $\Delta S/k_B$ and $\Delta U/k_BT_m$. In what follows, these terms are omitted from the analysis.

From Eqs. (1)-(4) for the liquid, and Eqs. (7) and (8) for the crystal, it follows

$$\Delta S(P = 0) = 3k_B\Delta \ln \theta_0 + S_{tr}, \tag{14}$$

$$\Delta U(P = 0) = \Delta\Phi_0 + U_{tr}. \tag{15}$$

The first term in ΔS is the leading (classical) term in $S^l_{vib} - S^c_{vib}$,

$$3k_B\Delta \ln \theta_0 = 3k_B[\ln \theta^c_0(V^c_m) - \ln \theta^l_0(V^l_m)]; \tag{16}$$

the first term in ΔU is the structural potential difference

$$\Delta\Phi_0 = \Phi^l_0(V^l_m) - \Phi^c_0(V^c_m); \tag{17}$$

and S_{tr} and U_{tr} are evaluated at V^l_m, T_m. The essential physical character of equilibrium melting is contained in the four terms explicit on the right sides of Eqs. (14) and (15). Our DFT evaluations of these terms are listed in Table IV.

Let us next examine the physical role of each term in melting at $P = 0$. Since the transit terms belong to the liquid alone, they are independent of the melting process, hence are entirely normal, with no contribution from the melting volume change. Moreover, because of the scaling properties of the transit free energy,[28] each quantity S_{tr}/k_B and U_{tr}/k_BT_m has a common magnitude for normal and anomalous elements alike. The transit contributions are graphed versus η in Figs. 4(a) and 4(b), where it is seen that each is essentially constant, the same for normal and anomalous melting and independent of η.

At this point, the entire anomalous contribution to melting at $P = 0$ has been isolated within the first terms on the right of Eqs. (14) and (15). Consider first the melting entropy, where the key is θ_0. For normal melting elements, the common electronic structure at a common V implies $\theta_0^c(V) \approx \theta_0^l(V)$, so that $3k_B\Delta \ln \theta_0$ results entirely from the melting volume change, and produces the volume change contribution to the normal melting distribution in Fig. 2. The same behavior is shown in Fig. 4(a) by the theoretical data for our set of normal melting elements, Na and Cu. In anomalous melting, the dominant effect is a significant decrease in θ_0 from crystal to liquid, caused by the electronic structure change, and this along with a small unresolved volume change contribution produces the higher-lying anomalous distribution in Fig. 2. The same behavior is shown in Fig. 4(a) by the theoretical data for Ga.

The situation with the internal energy is more complicated. The analysis of experimental energy data has not been done, because one cannot determine $\Delta\Phi_0$ from experimental data alone. However, $\Delta\Phi_0$ is subject to *a priori* calculation within the framework of V-T theory. For normal melting elements, $\Delta\Phi_0$ has contributions from both the structural change and the volume change, as indicated in Eq. (17). For Na and Cu, these contributions can be read directly from the calculated $\Phi_0(V)$ graphs.[14] The result is a characteristic normal-melting magnitude of $\Delta\Phi_0/k_BT_m$, as exemplified by Na and Cu in Fig. 4(b). For anomalous melting elements, $\Delta\Phi_0$ is *crucially different* because it is dominated by the change in electronic structure. Equation (17) is still correct, but it is not useful to attempt its decomposition into structural change and volume change contributions. However, the anomalous-melting $\Delta\Phi_0/k_BT_m$ is notably larger than the normal values, as exemplified by Ga in Fig. 4(b).

V. SUMMARY AND CONCLUSIONS

Our calculations of the structural and vibrational Hamiltonian parameters of crystal and liquid Ga are done with DFT. The entropy and internal energy of the crystal at melt, calculated from lattice dynamics theory, are in excellent agreement with experiment, as shown in Table II. Given the known accuracy of lattice dynamics, we take this agreement as validation of our computational procedures.

To find the liquid structure for a given element, a set of quenches is made to verify the uniformity of the random valleys that underly the liquid motion. With that established, the liquid vibrational properties can be calculated from a single (harmonically extended) valley. The procedure is illustrated for l-Ga in the Supplemental Material.[25] For l-Ga at melt, the theoretical entropy and internal energy are in good agreement with experiment, Table II, which we take as validation for using V-T theory for Ga. This conclusion is sustainable because, while the small transit contributions are determined by statistical mechanics and experimental data,[27,28] the strongly dominant structural and vibrational contributions (Table I) are calculated entirely from DFT.

In order to relate the melting analysis directly to the crystal and liquid phases at melt, the original constant-volume analysis (Ref. 13) is reformulated at $P = 0$ in Sec. III. The normal and anomalous distributions of $\Delta S(P = 0)$ remain clearly separated in Fig. 2. From the viewpoint of experiment, the fitted lines in Fig. 2 provide a template for classifying the melting of an element as normal or anomalous, and for measuring the anomalous character on the scale from Sn to Si. From the theoretical viewpoint, Fig. 2 is to be analyzed in terms of the atomic motional contributions to $\Delta S(P = 0)$. This analysis is shown in Fig. 4(a) for Na, Cu, and Ga, for the total motion (vibrational plus transit), and for the transit motion separately. The similarity of the entropy and energy analyses, Figs. 4(a) and 4(b), respectively, results from the condition $P = 0$ plus the scaling properties of the transit free energy. Our ultimate *theoretical* data in Figs. 4(a) and 4(b) display the same character seen for *experimental* data in Fig. 2.

To summarize the major conclusion of this study, let us make a qualitative description of the melting process, in terms of the structural potentials and nuclear motions of the equilibrium phases at melt. Ga will serve as our representative material. l-Ga is a NFE metal, and has the scaled transit free energy common to the elemental liquids we have so far studied.[14,27] Hence in Fig. 4, values of S_{tr}/k_B and U_{tr}/k_BT_m are common to Ga, Na, and Cu. Let us next consider a hypothetical NFE Ga crystal, for which crystal and liquid will have a common electronic structure, hence approximately the same internuclear forces at a common volume. The melting will be normal, and the melting parameters will lie near those graphed for Na and Cu in Fig. 4. Let us now consider the actual α-Ga crystal. Each atom in α-Ga is a partner in one covalent pair bond, while the remaining bonds are metallic. The covalent bonds alter α-Ga in three ways from NFE Ga, and produce corresponding changes in the melting process. First, the covalent bonds are stronger than metallic bonds, giving them higher vibrational frequencies and increasing θ_0^c, so that $3\Delta \ln \theta_0$ is much larger than the normal value as shown in Fig. 4(a). Second, the stronger covalent bonds lower Φ_0^c and increase $\Delta\Phi_0$, making $\Delta\Phi_0/k_BT_m$ much larger than the normal value as shown in Fig. 4(b). Finally, the covalent bonds are shorter than the metallic bonds, enforcing a low-coordination low-density crystal and making η negative, as shown in Figs. 4(a) and 4(b).

We note the present analysis can be applied to crystal–crystal transitions, where it will be simpler because crystals have no transits (see Eqs. (8) and (9)). The classification of crystal–crystal transitions as normal or anomalous applies equally well, according to whether the two phases have the same or different electronic structures.

ACKNOWLEDGMENTS

This research is supported by the Department of Energy under Contract No. DE-AC52-06NA25396. Many thanks go to Eric Chisolm and Anders Niklasson for helpful and encouraging discussions.

---

[1] S. Heathman, R. G. Haire, T. Le Bihan, A. Lindbaum, M. Idiri, P. Normile, S. Li, R. Ahuja, B. Johansson, and G. H. Lander, Science **309**, 110 (2005).

[2] Lattice vibrations contributions to the entropy generally dominate over those from electronic excitation or spin fluctuations, though the latter cannot be neglected in cases such as the α-γ transition of cerium (see e.g., Ref. 34).

[3] J. B. Neaton and N. W. Ashcroft, Nature **400**, 141 (1999).

[4] M. Hanfland, K. Syassen, N. E. Christensen, and D. L. Novikov, Nature **408**, 174 (2000).

[5] J. Feng, R. G. Hennig, N. W. Ashcroft, and R. Hoffmann, Nature **451**, 445 (2008).

[6] S. I. Simak, U. Häussermann, R. Ahuja, S. Lidin, and B. Johansson, Phys. Rev. Lett. **85**, 142 (2000).

[7] U. Häussermann, S. I. Simak, R. Ahuja, and B. Johansson, Phys. Rev. Lett. **90**, 065701 (2003).

[8] J. B. Neaton and N. W. Ashcroft, Phys. Rev. Lett. **86**, 2830 (2001).

[9] M. Hanfland, I. Loa, and K. Syassen, Phys. Rev. B **65**, 184109 (2002).

[10] K. Syassen, in *High Pressure Phenomena*, edited by R. J. Hemley, G. Chiarotti, M. Bernasconi, and L. Ulivi (IOS, Amsterdam, 2002) p. 251.

[11] E. Gregoryanz, O. Degtyareva, M. Somayazulu, R. J. Hemley, and H. K. Mao, Phys. Rev. Lett. **94**, 185502 (2005).

[12] J.-Y. Raty, E. Schwegler, and S. A. Bonev, Nature **449**, 448 (2007).

[13] D. C. Wallace, Proc. R. Soc. Lond. A **433**, 615 (1991).

[14] N. Bock, E. Holmström, T. B. Peery, R. Lizárraga, E. D. Chisolm, G. De Lorenzi-Venneri, and D. C. Wallace, Phys. Rev. B **82**, 144101 (2010).

[15] P. Ascarelli, Phys. Rev. **143**, 36 (1966).

[16] V. M. Nield, R. L. McGreevy, and M. G. Tucker, Journal of Physics: Condensed Matter **10**, 3293 (1998).

[17] E. L. Gromnitskaya, O. F. Yagafarov, O. V. Stalgorova, V. V. Brazhkin, and A. G. Lyapin, Phys. Rev. Lett. **98**, 165503 (2007).

[18] A. Lyapin, E. Gromnitskaya, O. Yagafarov, O. Stal'gorova, and V. Brazhkin, Journal of Experimental and Theoretical Physics **107**, 818 (2008).

[19] V. Heine, Journal of Physics C: Solid State Physics **1**, 222 (1968).

[20] V. Heine and D. Weaire, in *Solid State Physics*, Vol. 24, edited by H. Ehrenreich, F. Seitz, and D. Turnbull (Academic Press, 1970) pp. 249 – 463.

[21] J. Hafner and W. Jank, Phys. Rev. B **42**, 11530 (1990).

[22] X. G. Gong, G. L. Chiarotti, M. Parrinello, and E. Tosatti, Phys. Rev. B **43**, 14277 (1991).

[23] E. Voloshina, K. Rosciszewski, and B. Paulus, Phys. Rev. B **79**, 045113 (2009).

[24] J. Donohue, *The Structures of the Elements* (John Wiley and Sons, 1974).

[25] "See supplemental material at xyz for details.".

[26] D. C. Wallace, *Statistical Physics of Crystals and Liquids* (World Scientific, New Jersey, 2002).

[27] D. C. Wallace, E. D. Chisolm, and N. Bock, Phys. Rev. E **79**, 051201 (2009).

[28] D. C. Wallace, E. D. Chisolm, N. Bock, and G. De Lorenzi-Venneri, Phys. Rev. E **81**, 041201 (2010).

[29] O. Eriksson, J. M. Wills, and D. C. Wallace, Phys. Rev. B **46**, 5221 (1992).

[30] M. Born and K. Huang, *Dynamical Theory of Crystal Lattices* (Clarendon Press, Oxford, 1954).

[31] R. Hultgren, P. D. Desai, D. T. Hawkins, M. Gleiser, K. K. Kelley, and D. D. Wagman, *Selected Values of the Thermodynamic Properties of the Elements* (ASM, Metals Park, Ohio, 1973).

[32] M. W. Chase, Jr., C. A. Davies, J. R. Downey, Jr., D. J. Frurip, R. A. McDonald, and A. N. Syverud, J. Phys. Chem. Ref. Data **14** (1985), supplement 1.

[33] The value 353.1 for U^c of fcc Cu in Table V of Ref. 14 should be replaced by 360.1, the sum of the three terms in Table III. No conclusions are affected.

[34] B. Amadon, S. Biermann, A. Georges, and F. Aryasetiawan, Phys. Rev. Lett. **96**, 066402 (2006).